Research of Pattern Formation, edited by R. Takaki, pp. 329–341.

Chemically Driven Dynamic Patterns at an Oil-Water Interface: Wave Form Analysis and Computer Simulation

Shoichi KAI, Mustumaru MIKI, and Toshio MORI

Department of Electrical Engineering, Kyushu Institute of Technology, Tobata. Kitakyushu 804, Japan

Abstract. The quantitative wave profiles are experimentally obtained by use of image processing technique and compared with the results of the computer simulation of the model equation based on the diffusion reaction equation with drift terms. The profile obtained from the computer simulation well agrees with the experimental results most of which are described in detail in Part 1, where soliton-like, standing and traveling waves have been observed. However some aspects cannot be obtained by this model.

1. Introduction

In part 1 (Kai *et al.*, 1991), we have described mainly qualitative experiments and explanations. Past theoretical works on the Marangoni phenomena due to chemical reactions were done by several authors (see references in Part 1). However, they mainly concerned with the onset of the instability and were not interested of the wave profiles and their dynamical motions. Here we will describe more quantitative results of experiments and the simulations on their dynamical aspects.

2. Preparation

2.1 Experimental

Basic experimental procedures such as chemicals and containers have been already described in Part I (Kai *et al.*, 1991). Here we describe special equipment

for more quantitative observations. In order to observe dynamic changes and motions of waves in whole spatial area along a concentric container simultaneously, we use a cone-shaped mirror with an angle of 45 degrees as schematically shown in Fig. 1. Then The images are taken from the above by CCD (charge coupled device) TV camera which is connected to a video taperecorder (JVC-BR8600) and a personal computer (NEC, PC-9801 VM). A personal computer controls a video tape recorder and also reforms wave profiles to original forms from images on a cone-shaped mirror. An example is shown in Fig. 2. Figure 3 shows various wave profiles obtained by this technique. Figure 4 also shows a soliton-like behavior where one can observe collision of two waves and passing-through them. This motion can be often observed in the late stage of a reaction.

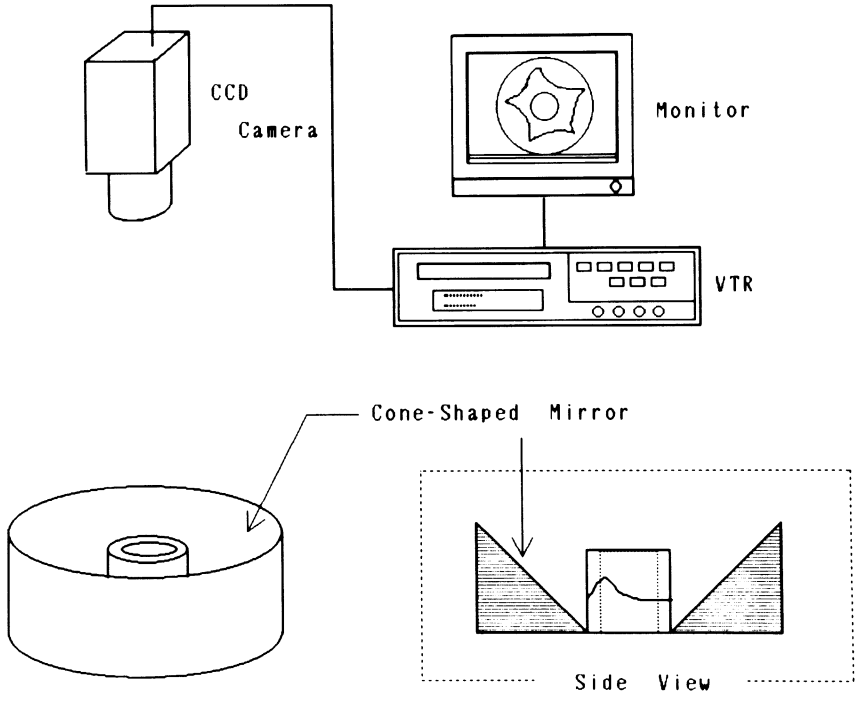

Fig. 1. Observation and analysing set-up for rotating waves.

2.2 Model equation

According to the chemical reaction and diffusion as described in Part I (Fig. 19), we consider the simplest reaction diffusion mechanism i.e., we introduce a simple switching mechanism in Fig. 5. The model equation is following.

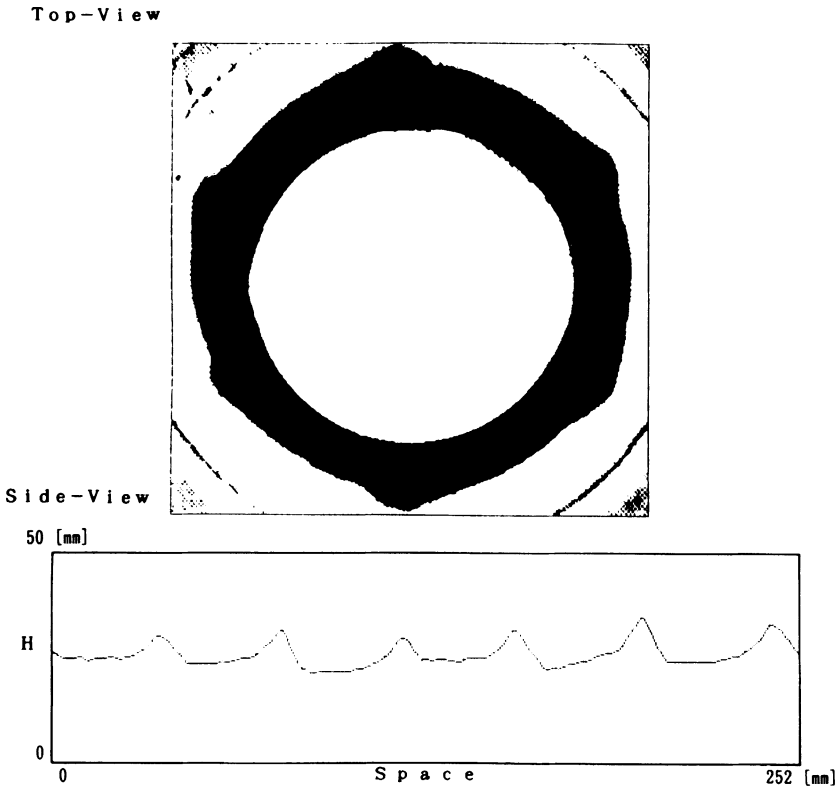

Fig. 2. Typical example of observed waves. Top figure: images on a cone-shaped mirror. Bottom figure: reformed waves by a computer after taking an image data.

$$\partial C_A / \partial t$$
$$= -kC_A C_B + D'_A \left(C_0 - C_A\right) + D_A \partial^2 C_A / \partial x^2 + v_o \partial C_A / \partial x + v_1 \left(\partial C_A / \partial x\right)^2 \quad (1)$$

Here C_A, C_B and C_0 are the concentration of surfactant ion, the concentration of I^- -ion and the initial concentration of surfactant ion at the interface respectively. k is the reaction rate constant. D_A and D'_A are the lateral diffusion constant in the interface and the effective diffusion constant from a bulk containing the boundary layer thickness. v_0 and v_1 express the drift terms coming from hydrodynamic flow effects and all hydrodynamic effects are included in these terms. The coordinate x indicates the space along the wall of a container in one dimension. Equation (1) is nondimensionalized as,

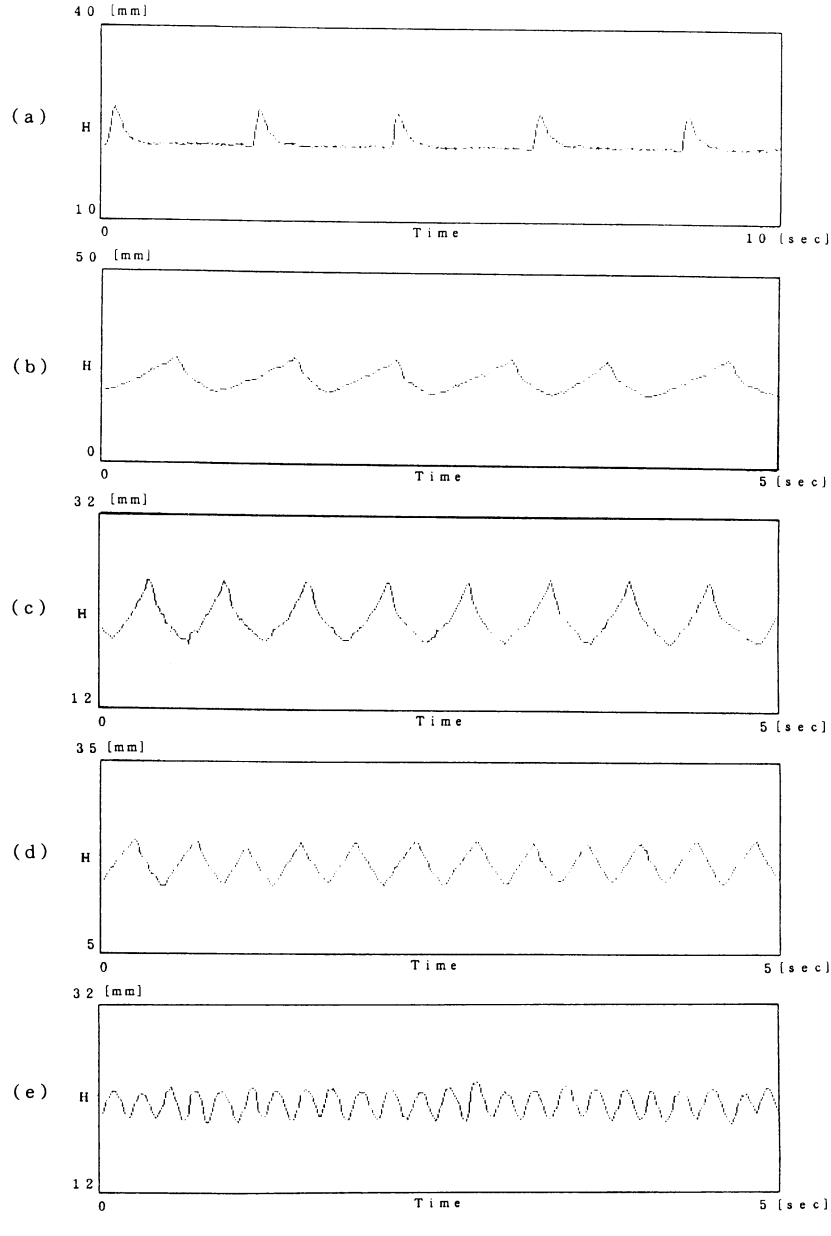

Fig. 3. Various waves observed in the present system. (a), (b) relaxation oscillation type (c) cusp-like (d) triangle (d) sinusoidal-like waves.

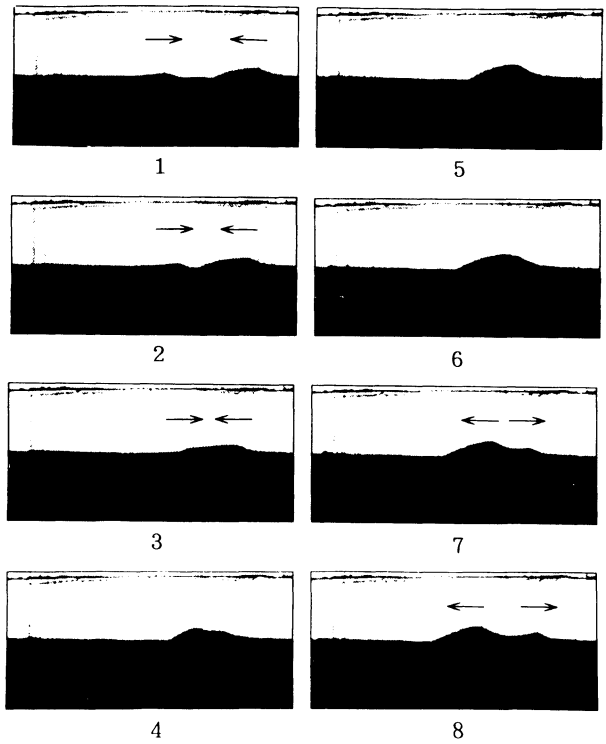

Fig. 4. Soliton like motion showing "pass-through each other".

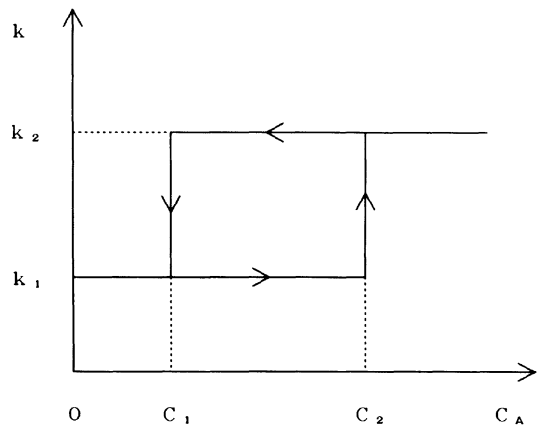

Fig. 5. Assumption for hysteresis of reaction rate k due to concentration C_A.

$$\partial C'_A / \partial t' = A - BC'_A C_0 + \alpha \partial^2 C'_A / \partial x'^2 + \beta \partial C'_A / \partial x' + \gamma \left(\partial C'_A / \partial x' \right)^2, \quad (2)$$

by $A = (l^2/D_A)D'_A$, $B = (l^2/D_A)(kC_B + D'_A)$, $\alpha = const.$, $\beta = \beta'(v_0 l/D_A)$ and $\gamma = \gamma'(v_1 C_0/D_A)$. Here $C'_A = C_A/C_0$, $t' = tD_A/l^2$ and $x' = x/l$. Hereafter we neglect a superscript ' of nondimension variables. α, β' and γ' are coefficients indicating contribution to the phenomenon. The surface tension II (dyn/cm) due to the concentration difference of a surfactant RAC is given by equation,

$$\Pi = 9.3 / \left(\log C_A / 2 + 1 \right) + 28, \quad (3)$$

obtained experimentally (Kai *et al.*, 1985). By the capirally effect caused by this surface tension, therefore, the height Δh (cm) of waves can be estimated as an order of centimeter from the relation,

$$\Delta h = \left(4 \cos\theta / \Delta pgl \right) \cdot \Pi. \quad (4)$$

Here Δp, g and l are the density difference (~0.3) between two fluids, the gravitational accelaration (980 cm/s^2) and the space width (1 to 5 mm) between container walls, respectively. θ is a contact angle (assumed to be ~0 when the surfactant exists.). The simulation has been done by use of difference equation form of Eq. (2). The space x is divided into 100 and each one is dominated by Eq. (2). Therefore, we have 100 linearly-coupled oscillators in space.

The initial conditions are set as follows. (1) The ion of RAC is uniformly distributed in space. (2) The initial perturbation is given only at one oscillator at the center. This corresponds to triggering. (3) The boundary condition is periodic. (4) $\Delta t = 5 \cdot 10^{-5}$. (5) The other parameters are used from actual experimental values: $C_0 = 1 \cdot 10^{-3}$ M, $C_B = 8 \cdot 10^{-3}$ M, $k_1 = 1$ (Ms)$^{-1}$, $k_2 = 5000$ (Ms)$^{-1}$, $D'_A = 1 s^{-1}$, $D_A = 0.05$ cm^2/s and $l = 10$ cm. The calculation is done by a personal computer (NEC PC-9801VX).

3. Result

Figure 6 shows the typical wave profile and the temporal sequencies of a wave motion obtained from the simulation. Here all temporal interval for display are chosen at 0.02 s. The initial perturbation is given at the center. In Fig. 6a, two waves which behave symmetrically are formed, travel to the opposite direction each other (noting to be a periodic boundary condition) and annihilate by collision. It shows typical property of dissipative waves. After collision no wave forms any more. This property is basically due to γ of the second order drift term. We call therefore this wave the trigger wave (TRW). In Fig. 6b, two waves nucleated by an initial triggering travel to the opposite direction each other. After their collision they pass

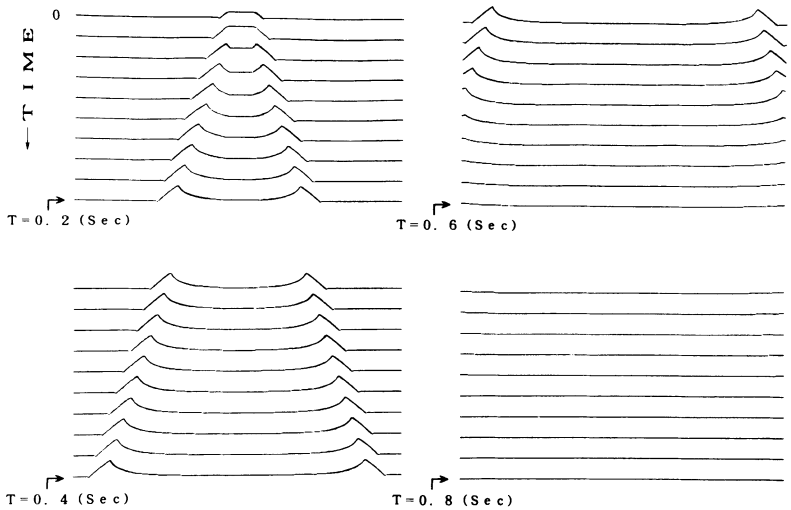

(a)

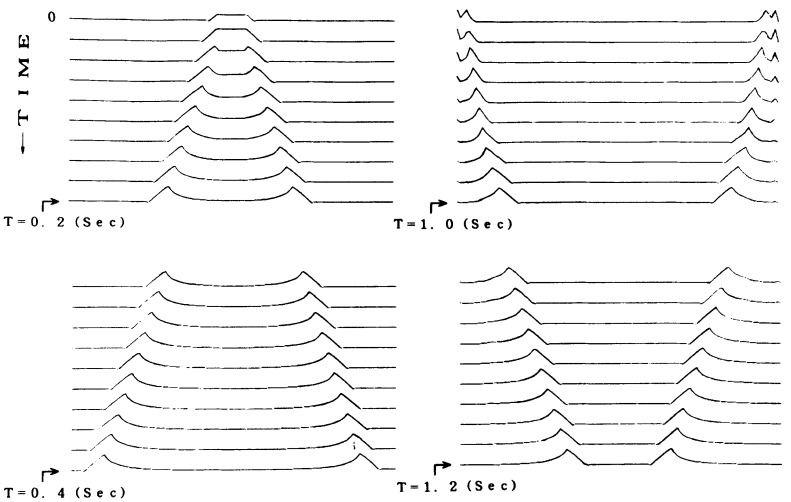

(b)

Fig. 6. Examples of computer simulation. (a) TRW (b) PTW.

Table 1. Classification of waves in α-β-γ parameter regions. (a) β = 0, (b) γ = 0, (c) α = 0.01. A(O)TW: asymmetrically (one direction) traveling wave ATRW: asymmetrically taveling triger wave TRW: triger wave SW: standing wave BW:bifurcation wave RAND: random wave N: no available to simulate ×: no wave.

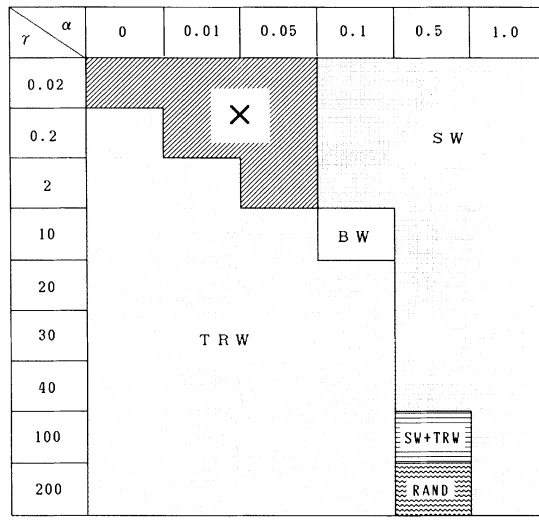

(a)

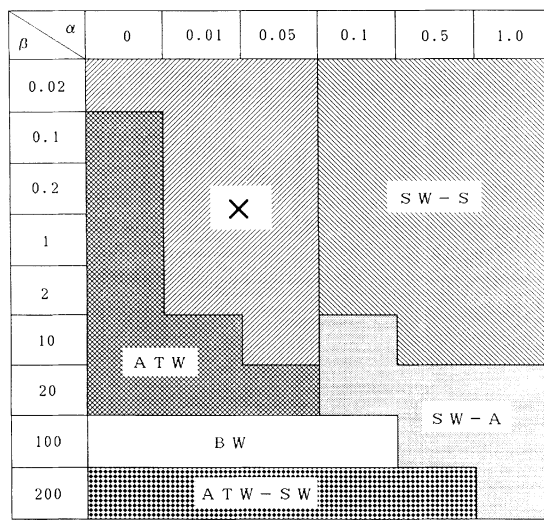

(b)

Table 1. continued.

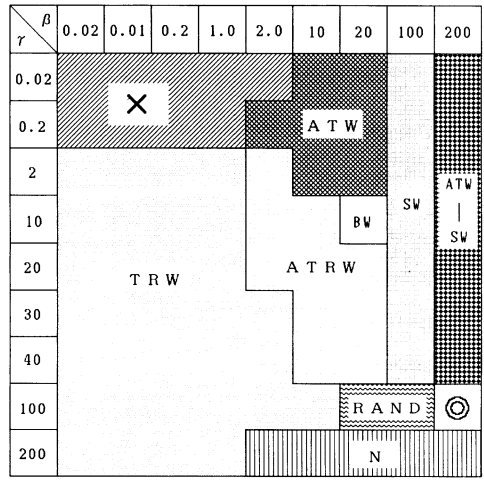

(c)

through without annihilation. This is repeated forever as long as chemicals are left. This behavior is well-known as one of a typical soliton, which is rather due to β of the first order term for drift. We call this the passing-through wave (PTW). One can note that the wave profile obtained from simulation is quite similar to the experimentally observed one. Since parameter regions for various motions are given in Table 1, we will not give detailed parameter values in each figure caption.

Figure 7 shows that TRW spontaneously bifurcates in a cascade way and annihilates by collision which make more complex state at $\beta = 0$. This is called the random wave (RAND). The larger the γ, in this case, the faster the traveling velocity of waves. When $\gamma = 0$ and $\beta \neq 0$, a motion is not symmetric and one wave is created by an initial triggering which travels to one direction as shown in Fig. 8 (A(O)TW). β expresses the traveling velocity. Increasing β, the waves self-bifurcate but never collide unlike a previous case. They change the velocities and finally become perfect standing waves from traveling waves. This is called the BUNKI (bifurcation in English) wave (BW) and the standing wave (SW), and expresses by "BW and SW" in Table 1.

When both β and γ are not zero, various non-symmetric behavior can be observed. A typical aspect is shown in Fig. 9. One notes here that due to non-symmetric property the waves do not disappear by collision. Instead, imediately after collision, the velocity is changed. However, later the velocity recovers to the initial value. When increasing β, waves often bifurcate and tend to be SW. We indicate this "SW-A" (asymmetric wave) in Table 1. Further, we could find a region

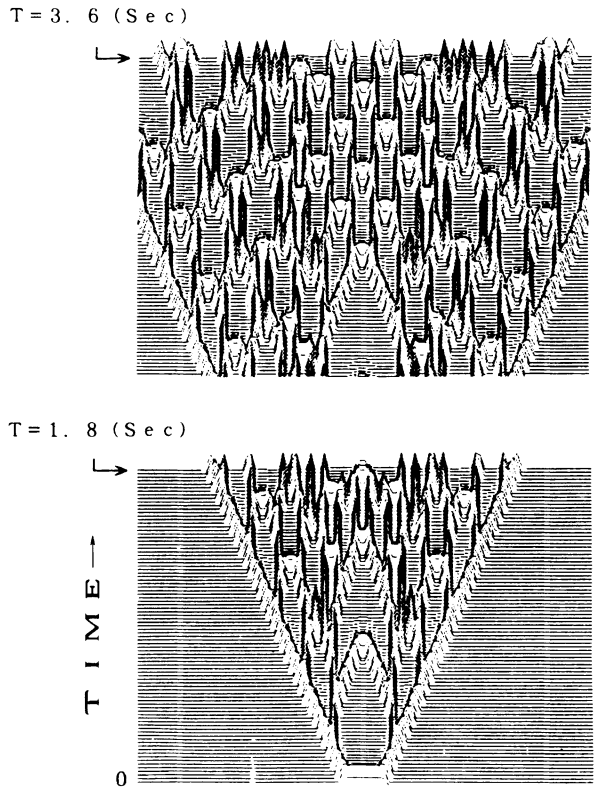

Fig. 7. Examples of BUNKI (bifurcation) wave (BW) ($\beta = 0$ and $\gamma \neq 0$). TW spontaneously bifurcate and annihilate with collision (TW to RAND).

where waves are intermittently formed (◎ in Table 1). For very large β and γ our simulation could not be possible because of too fast travels of waves.

In actual experiments, SW has never observed. On the other hand, while we actually observe for example both a cusp-like and triangle wave forms as shown in Fig. 3, no such profiles are available in our simulation (see Table 2).

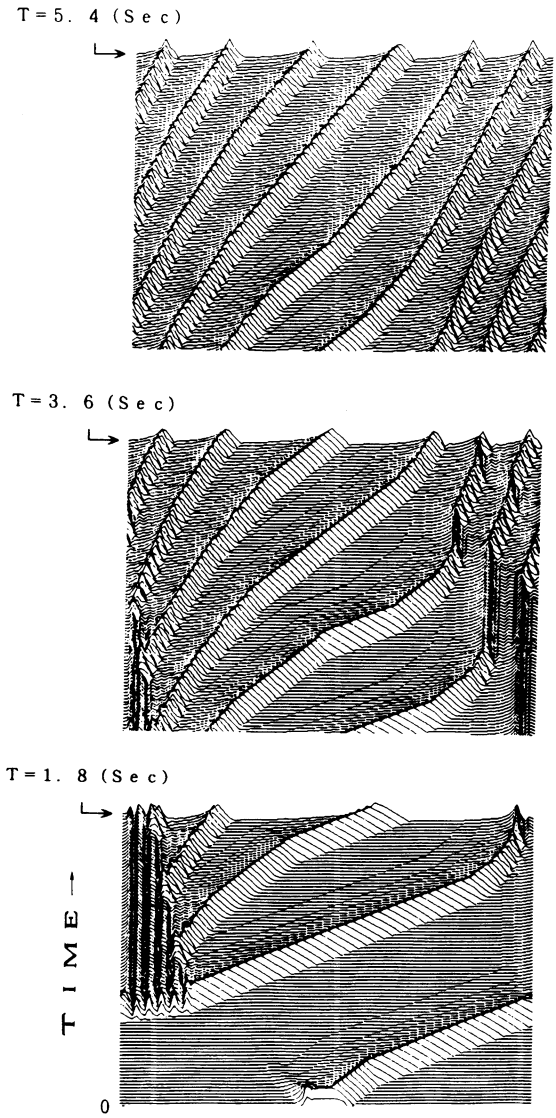

Fig. 8. Asymmetric motion (ATW: travel to one direction) to standing wave ($\beta \neq 0$ and $\gamma = 0$) (SW-A). No collision occurs.

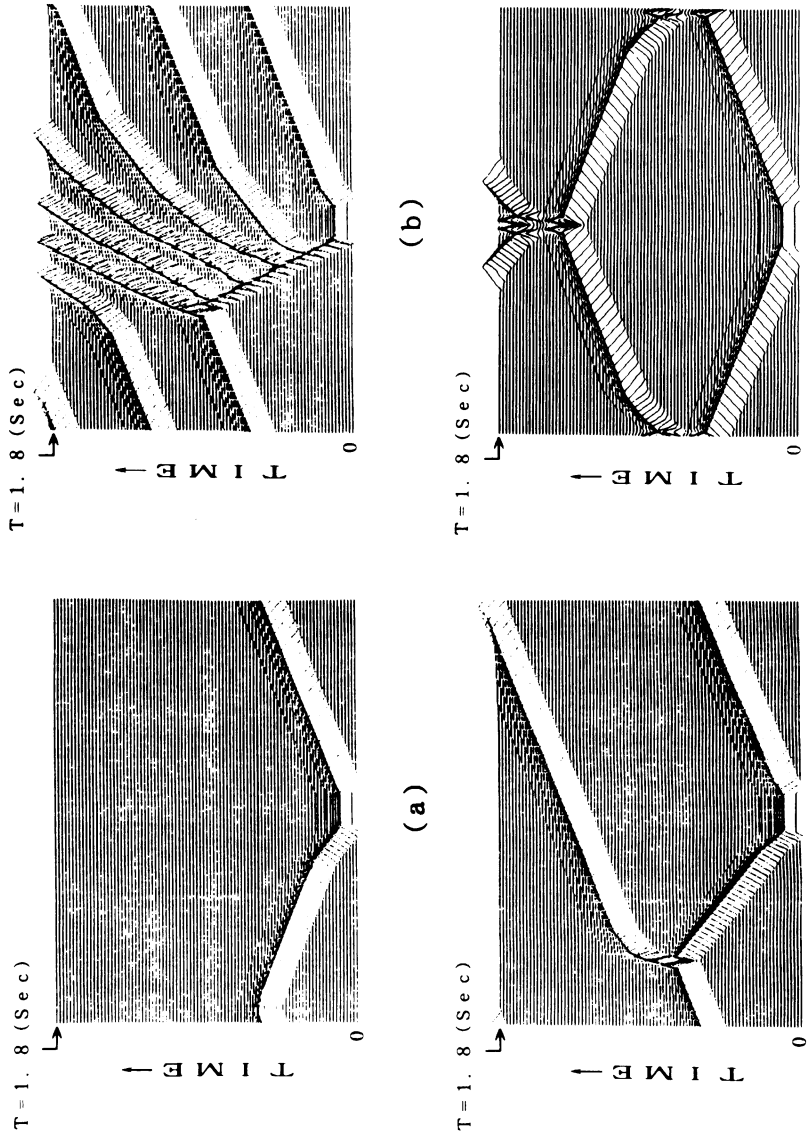

Fig. 9. Asymmetric motion and collision ($\beta, \gamma \neq 0$). (a) After collision, the velocity is changed. (b) Small additional waves can be seen.

Table 2. Comparison with simulation and experimental results. ○: observed ×: no observation.

Wave motion	Simulation	Experiment
ATW	○	○
ATRW	○	○
TRW	○	○
RAND	○	○
PTW	○	×
SW	○	×

4. Conclusion

The computer simulation of the present model equation, using the reaction diffusion equation, containing drift terms and the assumption of switching mechanism of reaction rate dependent on concentration, has well described the wave profile of relaxation-oscillation type and motions. Reasonable parameter values are used in calculation obtained from experimental facts. From the simulation the resulted value of height and form of waves show the corresponding value and profile observed in experiments. However, it cannot describe all experimental facts. The results are summarized in Table 2. The basic feature of the phenomenon can be explained by the present equation for an interface boundary layer.

More complete equation may be desired. Especially analytical introduction of drift terms from basic equations of this phenomenon will be needed, which we have automatically introduced in our equation regarding as the contribution from hydrodynamic effects. Most will be future subjects.

REFERENCES

Kai, S., Ooishi, E., and Imasaki, M. (1985), Experimental study of nonlinear waves on interface between two liquid phases with chemical reaction J. Phys. Soc. Jpn., **54**, 1974–1981.

Kai, S., Muller, S. C., Mori, T., and Miki, M. (1991), Chemically driven dynamic patterns at an oil-interface, in Research of Pattern Formation, edited by Takagi, R., KTK publisher, Tokyo; Physica (1991), **D50**, 412–428.